Photophysical Dynamics of Single Molecules Studied by Spectrally-Resolved Fluorescence Lifetime Imaging Microscopy (SFLIM)

Philip Tinnefeld, Dirk-Peter Herten, and Markus Sauer*

Physikalisch-Chemisches Institut, Universität Heidelberg, Im Neuenheimer Feld 253, 69120 Heidelberg, Germany

Received: January 29, 2001; In Final Form: April 26, 2001

A new scanning technique for simultaneous recording of intensity, fluorescence lifetime, and spectral information with single molecule sensitivity is presented. We investigated and compared the photophysical parameters of single oxazine (JA242), rhodamine (JF9), and carbocyanine (Cy5) derivatives adsorbed on glass surfaces under air-equilibrated conditions. The obtained results demonstrate that spectrally resolved fluorescence lifetime imaging microscopy (SFLIM) is ideally suited to reveal subpopulations in inhomogeneous samples and mixtures. To obtain a more detailed insight into the underlying fluorescence dynamics of single molecules, the fluorescence characteristics of the three different chromophores were studied positioning isolated molecules in the laser focus. Two detectors with two PC plug-in cards for time-correlated single-photon counting (TCSPC) were utilized to monitor fluorescence intensity, lifetime, and spectral information simultaneously with single-molecule sensitivity and microseconds to milliseconds time resolution. Discrete jumps in fluorescence intensity from single molecules which lacked spectral diffusion and changes in radiative lifetime have been observed with correlation times (triplet lifetimes) spanning several orders of magnitude (from 2 μs for the rhodamine derivative up to several seconds for the oxazine dye) and amplitude. For the carbocyanine derivative Cy5, fast spectral fluctuations to red-shifted dim-states which appear partly as off-states with a lifetime in the millisecond range were determined. In addition, these dim-states exhibit the same radiative decay rate of ~2 ns as the normal on-state. Our results imply that a direct correlation between the radiative decay time and spectral fluctuations is not necessarily given in each of the three chromophores. Both parameters seem to be independent characteristic of each individual molecule. About 5−15% of all molecules independent of the dye structure, respectively, exhibited a constant emission spectrum but strong fluctuations in fluorescence lifetime directly correlated to the intensity. The results indicate that a combined analysis of emission spectrum, intensity and radiative decay rate is a valuable approach for classification and quantification of the underlying photophysical dynamics.

Introduction

The knowledge obtained from fundamental single-molecule studies under ambient conditions at interfaces[1−5] or in solution[6−10] has been successfully transposed into practice of single-molecule microscopy and spectroscopy to study the conformational dynamics of individual biomolecules or to probe the dynamics of the local environment of a chromophore.[11−19] The ability to detect and identify individual fluorescent molecules with high signal-to-background ratios enabled the observation of various phenomena that are hidden in ensemble measurements due to averaging. Among these phenomena are fluorescence intensity fluctuations due to spectral diffusion[20−27] or triplet[22,28−30] and rotational jumps,[31−33] as well as photon (anti-)bunching.[34−38] Very recently,[39] even fluctuations in fluorescence lifetime of single fluorophores have been investigated with millisecond time resolution.

With respect to the used time-resolution intensity fluctuations are often observed as discrete intensity jumps from an "on" intensity level with high count rate to a "dim" or "off" intensity level with reduced or background count rate, respectively. This effect which has often been denoted as "blinking" is commonly accepted as an obvious criterion for a single-chromophore system. The blinking behavior is not restricted to chromophores attached at interfaces or immobilized in polymers, even in solution single chromophores attached to biomolecules such as DNA[40,41] or proteins[42] show distinct changes in intensity and spectrum which might appear as off-states.

Typically, the temporal and spatial fluctuations of the local environment around a single chromophore have been monitored by recording the fluorescence intensity and spectrum or polarization. It has been shown that little, if any, correlation between spectral width, position, and intensity exists. Each measured parameter of a single chromophore appeared to be an independent measure of the molecule's configuration or local environment.[26] However, it is still discussed whether the observed variations are due to inhomogeneous environmental distributions or insufficient sampling time due to rapid photobleaching.[24,28] Furthermore, it is not clear whether all classes of chromophores exhibit the same photophysical dynamics or if the dynamics is rather controlled by the chromophore structure itself. We therefore investigated and compared the fluorescence characteristics of three different classes of chromophores at the single-molecule

* Corresponding author. Phone: +49-6221-548460. Fax: +49-6221-544255. E-mail: sauer@urz.uni-heidelberg.de.

10.1021/jp010365l CCC: $20.00
Published on Web 08/03/2001

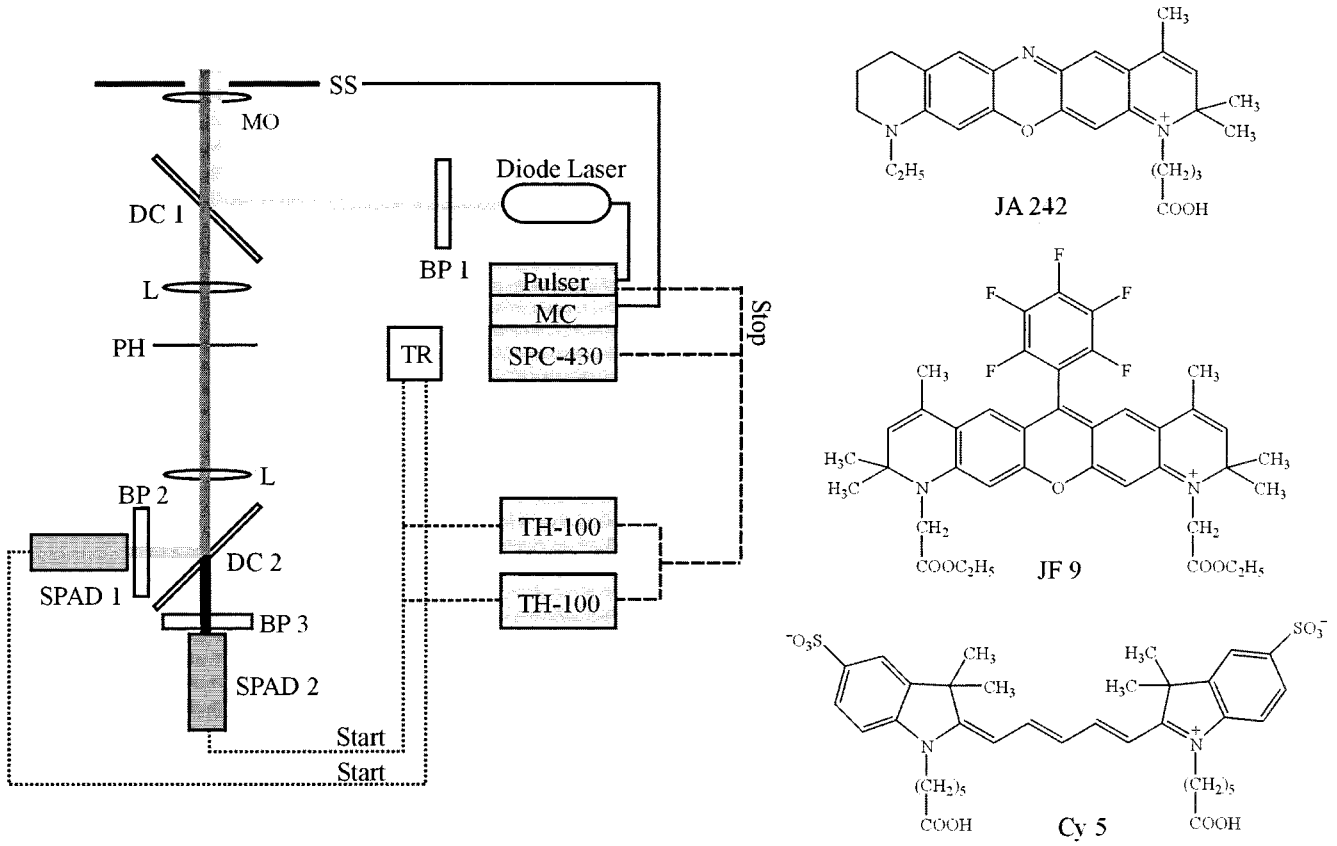

Figure 1. Schematic diagram of setup and molecular structure of the investigated dyes. SS: scanning stage. MC: motion controller. TR: time router. MO: microscope objective. DC: dichroic beam splitter. L: lense. PH: pinhole. BP: band-pass filter. SPAD: single-photon avalanche diode.

level: a rhodamine derivative (JF9), an oxazine derivative (JA242), and a carbocyanine derivative (Cy5) (Figure 1).

To get information about the relation between fluorescence fluctuations and emission yield of the chromophore we developed a method to measure the fluorescence lifetime of single molecules applying time-correlated single-photon counting (TCSPC) on two spectrally resolved detectors. This method allows the simultaneous recording of fluorescence lifetime and emission maximum in the micro- to millisecond time range.[43] With this technique, the question whether spectral jumps (spontaneous or light-driven) to a new resonance frequency are connected with changes in the excited-state kinetics can be answered.

Generally, spectral fluctuations have been attributed to transitions between different potential minima of the molecule's energy landscape. Among these are transitions due to changes of the nuclear coordinates within the chromophore backbone itself, i.e., cis/trans isomerization in case of carbocyanine dyes such as $DiIC_{18}$, or changes in the intermolecular coordinates released by the interacting environment.[21,25,26]

In this communication we want to demonstrate that spectrally- and time-resolved fluorescence detection of individual chromophores of different classes of dyes can contribute significantly to a better understanding of fluctuations in photophysical properties of single molecules.

Experimental and Methods

The fluorescent dye Cy5 was purchased from Amersham Life Science (Braunschweig, Germany). The rhodamine derivative JF9 and the oxazine derivative JA242 are kindly provided by K. H. Drexhage and J. Arden-Jacob (Universität-Gesamthochschule Siegen). The dyes were purified on a RP18-column using a gradient of 0−75% acetonitrile in 0.1 M aqueous triethylammonium acetate (TEAA) prior to use.

Corrected steady-state fluorescence spectra were measured in standard quartz cuvettes using an LS100 spectrometer (PTI, Canada). Ensemble fluorescence lifetimes were determined from 10^{-8} M solutions of the dyes at the emission maxima using a pulsed diode laser emitting at 635 nm as excitation source and time-correlated single-photon counting (TCSPC) with an IBH spectrometer (model 5000MC; Glasgow, Scotland). To exclude polarization effects, the fluorescence was recorded under the magic angle (54.7°).

For single-molecule imaging the dyes were adsorbed on standard cover slides with a thickness of 170 μm. Before use the cover slides were carefully cleaned with 5% hydrofluoric acid in water for 5 min then treated with a 0.1% aqueous solution of 3-aminopropyl-triethoxysilane (APS) for 5 min followed by a washing step with water and dried under nitrogen prior to use. A treatment with 10^{-10} M solutions of the dyes generally yielded an areal density of less than 1 molecule per μm^2. All single-molecule experiments were performed at room temperature.

Figure 1 gives a schematic diagram of the setup used for confocal time-correlated single-photon counting on two spectrally separated detectors. For excitation a pulsed laser diode with a center wavelength of 635 nm, a repetition rate of 64 MHz, and a pulse length of less than 100 ps (PDL800; Picoquant, Berlin, Germany) was used. The elliptical shape of the laser beam profile was converted into a circular (Gaussian-like) profile by the use of two cylindrical lenses. The collimated

laser beam was spectrally filtered by an excitation filter (639DF9; Omega Optics, Brattleboro, VT) and directed into an inverted microscope (Axiovert 100TV; Zeiss, Germany) via the backport. Within the microscope the beam was coupled into the microscope objective (100x, NA = 1.4; Nikon, Japan) by a dichroic beam splitter (645DMLP; Omega Optics, Brattleboro, VT) and focused onto the upper surface of the cover slide. The average excitation power was adjusted to 0.25−5 kW/cm^2 at the sample. Fluorescence light emitted by the sample was collected by the objective and focused through the TV outlet of the microscope onto a 50 or 100 μm pinhole. Fluorescence light passing the pinhole was spectrally separated by a nonpolarizing dichroic beam splitter (670DMLP; Omega Optics, Brattleboro, VT) and imaged onto the active area of two avalanche photodiodes (AQR-14; EG&G, Canada). The reflected light reaching detector 1 was filtered by two band-pass filters (685HQ70; AF Analyzentechnik, Tübingen, Germany and 660DF60; Omega Optics, Brattleboro, VT), whereas the transmitted light was filtered by a single band-pass filter (690DF60; Omega Optics, Brattleboro,VT) in front of detector 2.

For generation of spectrally resolved fluorescence lifetime images of single molecules the microscope was equipped with a motion controller driven *x*,*y*-microscope stage (SCAN 100 × 100, MC2000; Märzhäuser, Wetzlar, Germany). The signals of the two avalanche photodiodes were fed into the router of a TCSPC PC interface card (SPC-430; Becker&Hickl, Berlin, Germany) to acquire time-resolved data.[44] For synchronization of scanning and time-correlated single-photon counting, a Windows 32-based software was developed.[39] The fluorescence intensity and lifetime images on both detectors were recorded using a 50 μm pinhole at a resolution of 50 nm/pixel and a collection time of 7 ms/pixel. The spot size of the sample molecules in the resulting images was diffraction limited (~310 nm).

To measure fluctuations in fluorescence lifetime, intensity and spectrum with time molecules chosen from an image scan were positioned in the laser focus with the *x*,*y*-scanning stage. The photon counts detected on both detectors were registered with two PC plug-in cards for on-line TCSPC (TimeHarp100; Picoquant, Berlin, Germany) using the time-tagged time-resolved (TTTR) mode. This mode allows the registration of a detected photon on two independent time scales: (a) the absolute arrival time with a resolution of 100 ns and (b) the distance to the previous laser pulse with a time resolution of 37 ps/channel. The absolute arrival times of both detectors were used to construct multichannel-scalar (MCS) traces with arbitrary time resolution. The microscopic arrival time can be collected in histograms from which information about the fluorescence lifetime is obtained. The instrumental response function (IRF) of the entire system was measured to be ~400 ps fwhm. This arrangement enables theoretically the monitoring of fast (μs-ms) changes in fluorescence lifetime and spectrum. However, it should be pointed out that the obtainable time resolution (especially for fluorescence lifetime determination) strongly depends on the photon count statistics. To monitor fluctuations in fluorescence lifetime we used a sliding-scale analysis.[45] In a sliding-scale analysis, the signal trace of fluorescence arrival times is binned into a series of fluorescence decay histograms with a constant number of photon counts. Throughout this article we used 500 subsequent photon counts for the determination of the fluorescence lifetime and moved this window photon count by photon count over the whole data set. For efficient determination of fluorescence lifetimes with low photon count statistics we applied a maximum likelihood estimator (MLE)-algorithm using the following relation:[46,47]

$$\frac{\omega}{1-e^{-\omega/\tau}} - \frac{m\omega}{e^{m\omega/\tau}-1} = \frac{\sum_{i=1}^{m} i\omega N_i}{N} \qquad (1)$$

Here N represents the number of photon counts taken into account. The sum runs over m bins of width ω, with the ith bin containing N_i counts. To estimate the fluorescence lifetime τ, only a portion of m channels of width ω were used. Typically, a data window of about 10 ns starting ~370 ps behind the maximum channel was used. Equation 1 was numerically solved with respect to the fluorescence lifetime τ using Newtons algorithm. It should be mentioned that eq 1 holds only for monoexponential decays disregarding the convolution with the laser pulse.

TABLE 1: Spectroscopic Properties of the Rhodamine JF9, the Oxazine JA242, and the Carbocyanine Dye Cy5 in Ethanol and Water

		λ_{abs}(nm)	λ_{em}(nm)	τ (ns)	χ^2
JA242	H_2O	664	682	1.93	1.021
	C_2H_5OH	658	678	3.08	0.996
JF9	H_2O	630	652	3.86	1.073
	C_2H_5OH	632	657	4.07	1.013
Cy5	H_2O	651	670	0.98	1.009
	C_2H_5OH	652	672	1.42	1.038

Results and Discussion

Spectrally Resolved Fluorescence Lifetime Imaging. To investigate and to compare the influence of the dye structure on the fluorescence fluctuations of single molecules, we used three different chromophores: a rhodamine (JF9), an oxazine (JA242) and a carbocyanine dye (Cy5). In all three dyes, the π-electron distribution can be described approximately by two mesomeric structures, in which the positive charge is located on either of the two nitrogen atoms (Figure 1). Thus in these dyes there is no permanent electric dipole moment parallel to the long axis of the molecule in neither the ground nor the excited state.[48] Because the dipole moment does not change upon excitation, the absorption maximum shows only little dependence on the polarity of the solvent (Table 1). Due to the incorporation of the amino groups in rigid six-membered rings, the rhodamine derivative JF9 exhibits a fluorescence efficiency close to unity nearly independent of solvent polarity and temperature.[49] The red absorbing rhodamine derivative JF9 was derived from a "classical" rhodamine dye by an exchange of the carboxyphenyl substituent by an electron-accepting group (pentafluorophenyl group) at the central carbon (position 9) of the chromophore. The introduction of an electron-accepting group at position 9 of the xanthene chromophore has an effect similar to the introduction of a more electronegative atom (as in case of the oxazine derivative): the absorption and emission spectra shift toward the red wavelength range. Through the introduction of double bonds in the nitrogen-containing rings, the absorption and emission maxima are additionally shifted to longer wavelengths.[49] Hence, the three dyes can be excited with a pulsed diode laser emitting at 635 nm but exhibit distinct fluorescence emission maxima and lifetime (Table 1). In contrast to the relatively rigid structure of rhodamine and oxazine derivatives, the carbocyanine dye Cy5 exhibits a flexible backbone allowing a twist about the conjugated bridge. Recently,[50] it was shown that the cis configuration exhibits if at

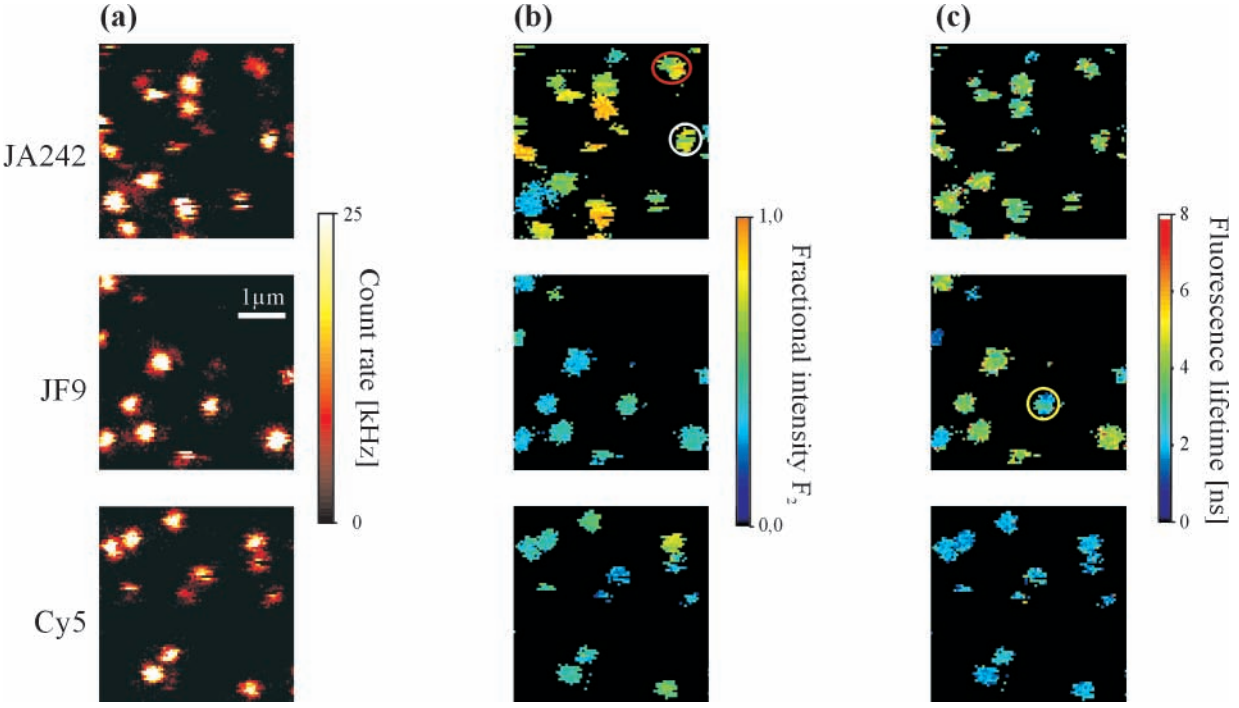

Figure 2. Scanning confocal fluorescence images of single JF9, JA242, and Cy5 molecules on dry glass surface (50 μm pinhole, 250 W/cm^2). The samples were scanned from top to bottom and from left to right with a resolution of 50 nm/pixel (7 ms integration time per pixel). **(a)** Fluorescence intensity image (detector 1 + detector 2). **(b)** Fractional intensity image (F_2-image) recorded at detector 2, $F_2 = I_2/(I_1 + I_2)$. **(c)** Fluorescence lifetime image (τ-image) calculated from the overall photon counts detected on both detectors.

all only weak emission. The rate constant for cis/trans-isomerization in water was measured to be 2.5×10^7 s^{-1} under moderate excitation conditions (>10kW/cm^2).

Scanning confocal fluorescence intensity images obtained from single JA242, JF9 and Cy5 molecules adsorbed on silanized cover slides are shown in Figure 2a. The images exhibit diffraction limited spots resulting from individual fluorescent dye molecules with overall count rates (detector 1 + detector 2) of up to 30 kHz at an excitation power of 250 W/cm^2. As indicated by the presence of several isolated dark pixels within the bright spots, the molecules undergo discrete photochemistry like blinking and digital photobleaching. From the fluorescence intensity registered at both detectors (I_1 and I_2) we calculated the fractional intensity F_2 at detector 2, $F_2 = I_2/(I_1 + I_2)$ for each pixel as a measure for the emission maximum (Figure 2b). Fluorescence lifetime τ-images (Figure 2c) were generated from the overall photon counts detected on both detectors using the MLE-algorithm described in the Experimental Section. In the resulting F_2- and τ-images, pixels corresponding to an overall count rate of less than 3 kHz were excluded.

While the intensity images (Figure 2a) exhibit almost similar intensities and photophysics, the F_2-images (Figure 2b) clearly indicate different emission maxima of the dyes. For example, JF9 molecules appear to exhibit relatively homogeneous spectral characteristics, whereas the F_2-values obtained for single oxazine derivative molecules (JA242) indicate a relatively broad spectral distribution. Molecules that change their emission spectrum during the image acquisition are evident, e.g., the JA242 molecule in the white circle at the right-hand side in Figure 2b. As shown in the red circle at the top right corner in Figure 2b, spectrally and time-resolved single-molecule detection can also help to distinguish a single-molecule from two or more closely spaced molecules with different spectra or lifetime. Therefore, the applied technique can also be used for high-resolution multicolor or multilifetime colocalization or high precision distance measurements.[51,52] As can be seen from the fluorescence lifetime images (Figure 2c), Cy5 molecules exhibit an almost constant fluorescence lifetime of ~2 ns. The fluorescence lifetimes measured from single rhodamine and oxazine derivatives are comparable longer with a broader distribution. As indicated in the τ-images, some molecules change their fluorescence lifetime during the image acquisition (for example the JF9 molecule in the yellow circle). Comparison of the F_2- and τ-images reveals several molecules that exhibit different τ but the same F_2-values or vice versa, i.e., obviously no correlation between spectrum and lifetime.

For further analysis we calculated the spot-integrated characteristics, i.e. more than 450 spots were analyzed for each dye by adding up all photon counts collected per single dye molecule. When two molecules were located too close (for example the molecules in the red circle in Figure 2b), they were excluded from the statistics. To estimate the emission maximum from the measured F_2-values we used the overall transmission efficiency of the filter set for both detectors and a model absorption and emission spectrum (Figure 3a). The emission spectrum was shifted through the transmission curve nm by nm to calculate the expected corresponding fractional intensity F_2. The resulting curve attaches an emission maximum in wavelengths to a F_2-value (Figure 3b). Here it should be pointed out that the position of the slope of the curve shown in Figure 3b is mainly influenced by the angular positions of the dichroic beam splitters. However, differences or fluctuations in emission maxima can be easily estimated if we assume comparable shapes of the spectra.

Another important point which has to be considered are the different absorption cross sections of the dyes at the excitation wavelength (635 nm). Assuming a constant Stokes shift of 20 nm for the investigated dyes (see Table 1) and comparable shapes of the absorption spectra, the excitation efficiency and detection probability of fluorescence photons on both detectors for different absorption and emission maxima can be evaluated. With these assumptions we calculated the relative detection

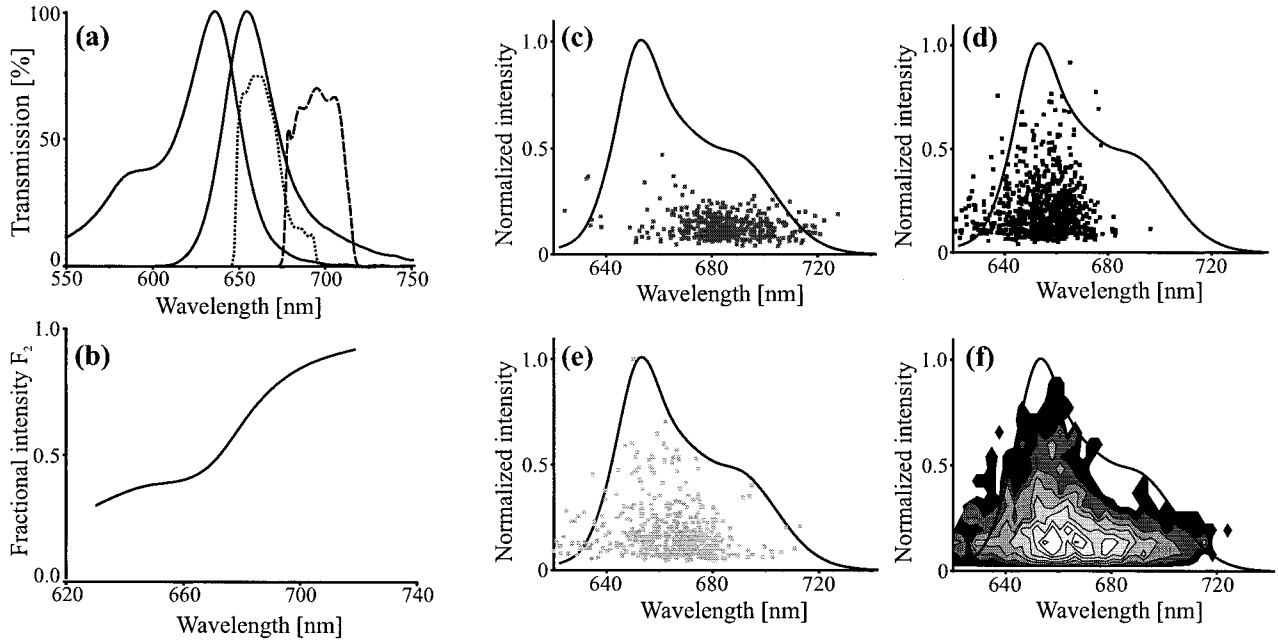

Figure 3. Relative detection sensitivity of the applied setup and distributions of the spot-integratedemission maxima of the dyes. **(a)** Overall transmission efficiency of the filter set for both detectors and model absorption and emission spectrum used for calculation of the detection sensitivity. **(**b**)** Fractional intensity F_2 and corresponding emission maximum calculated from the model spectra and the transmission efficiency of the filters. Wavelength dependent relative detection sensitivity and normalized scatter plots of the spot-integrated emission maxima of the dyes **(**c**)** JA242, **(**d**)** JF9, **(**e**)** Cy5, and **(**f**)** all three dyes together.

sensitivity of the applied setup at different emission maxima (Figure 3c−f). This procedure allows to monitor spontaneous changes in emission yield of a single dye as well as to compare the overall detection sensitivity of the setup for different dyes. Figure 3c−e present scatter plots of the spot-integrated emission maxima (calculated from the F_2-values) versus fluorescence intensity obtained from single JA242, JF9, and Cy5 dyes. Figure 3c−e clearly demonstrate that the applied setup exhibits a different detection sensitivity for each chromophore. While for JF9 molecules on an average 5000 photon counts have been detected, we obtained on an average 4400 photon counts for Cy5 and only 3200 for JA242 spots, respectively. However, if we correct for both, the different absorption cross section of the dyes at the excitation wavelength and the transmission efficiency of the filter set we obtain comparable fluorescence intensities from single JA242, JF9, and Cy5 molecules adsorbed on glass (Figure 4a). Normalized histograms of the spot-integrated corrected emission maxima obtained from single molecules are shown in Figure 4b. With exception of the Cy5 emission maxima distribution, the distributions obtained from rhodamine (JF9) and oxazine (JA242) molecules describe satisfactorily the emission curves obtained from ensemble measurements. Nevertheless, it should be pointed out that the applied technique is fairly sensitive to changes in the emission maximum but less suited to measure absolute values.

To test the homogeneity of the excited-state kinetics spot-integrated fluorescence lifetimes of the dyes were plotted versus their frequency and fitted by three Gaussians (Figure 4c). The fluorescence lifetime of 2.00 ± 0.34 ns measured for single Cy5 molecules on dry surface is definitely longer than measured from an ensemble in solution (see Table 1) and might be explained by a reduced flexibility of the polymethine backbone in Cy5 thereby increasing the excited-state lifetime. JF9 molecules exhibit nearly the same fluorescence lifetime as measured in solution (3.99 ± 0.83 ns). In contrast, the oxazine molecules show fluorescence lifetimes of 3.67 ± 0.74 ns, comparable to the value obtained in ethanol but definitely longer than in aqueous surrounding. This striking behavior might be triggered by the experimental conditions, i.e., the dry surface. It is known that the quanta of hydrogen stretching vibrations have the highest energies in organic dyes, and thus hydrogen vibrations and subsequent energy transfer to vibrations of solvent molecules are very likely to contribute to internal conversion.[48,49] Hence, an aqueous surrounding might significantly shorten the measured fluorescence lifetime. This mechanism is of minor importance in dyes that fluoresce in the visible range but becomes increasingly effective with decreasing energy difference between S_1 and S_0. In addition, the degree of this effect is strongly controlled by the dye structure itself and the microscopic environment of the fluorophore.[49]

The measured relatively broad distributions in fluorescence lifetimes of single molecules cannot be explained by low photon count statistics. On average, a few thousand photon counts were used to calculate the fluorescence lifetime via the MLE-algorithm. However, the dielectric interface modifies the radiative component of the excited-state lifetime due to the boundary conditions of the radiated field.[5,53] For example, for a dipole on the air side of the glass surface, the radiative lifetime is longer for a parallel emission dipole. Using a glass−air interface, the fluorescence lifetime recorded from a molecule with a parallel oriented emission dipole is expected to be ∼2 times that of a molecule oriented perpendicular to the surface.[54] In addition, a higher signal is obtained from a parallel emission dipole. With regard to these theoretical considerations, the measured lifetime distributions appear to be relatively narrow, indicating comparable orientations of the molecules on the glass surface.

To get more insight into the relation between emission maximum, fluorescence intensity, and fluorescence lifetime of single chromophores we constructed scatter plots (Figure 4d,e). The scatter plots indicate, if at all, only little correlation between fluorescence lifetime, emission maximum, and overall spot-integrated fluorescence intensity. As mentioned above, differences in fluorescence lifetime that do not correlate with the

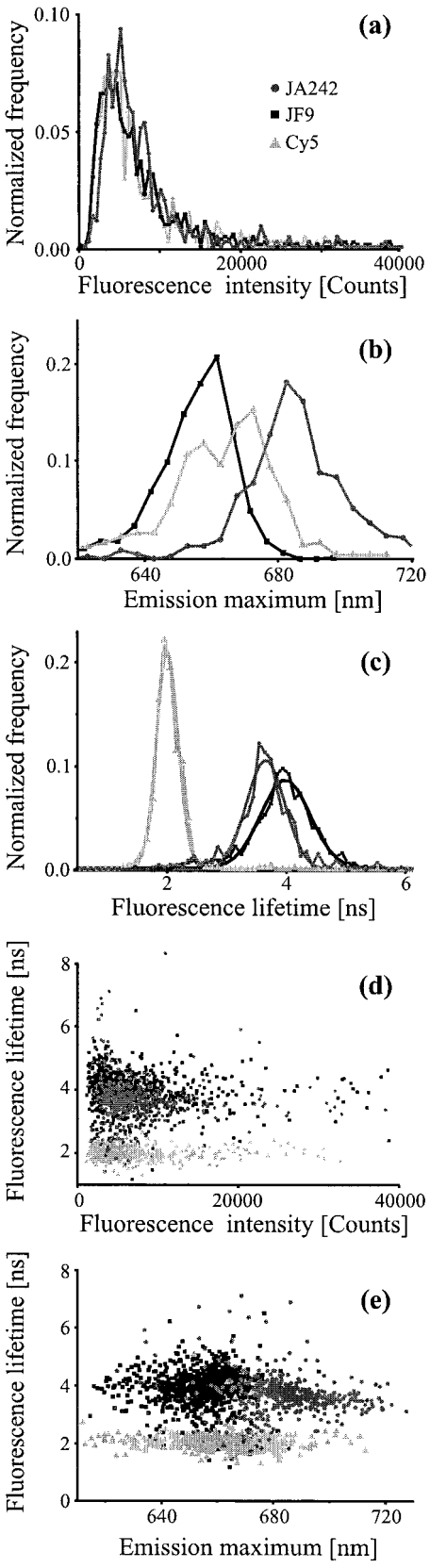

Figure 4. Spot-integrated photophysical characteristics of single JA242, JF9, and Cy5 molecules. **(**a**)** Normalized and corrected overall fluorescence intensity distribution, **(**b**)** normalized distribution of calculated emission maxima, **(**c**)** fluorescence lifetime distribution, **(**d**)** scatter plot of overall fluorescence intensity recorded on both detectors versus fluorescence lifetime, and **(e)** scatter plot of calculated emission maxima versus fluorescence lifetime.

TABLE 2: Off-State Rate Constants and Transition Yields of Single JA242, JF9, and Cy5 Molecules Determined from Autocorrelation Analysis of the Fluorescence Intensity

	JA242	JF9	Cy5
detected photon counts[a]	77.000	82.000	30.000
fluorescence lifetime τ (ns)	3.67 ± 0.74	3.99 ± 0.83	2.00 ± 0.34
triplet lifetime τ_T (ms)	1−150	0.002−0.007[b]	0.01−0.15
off-time τ_{off} (ms)			0.5−5
Triplet yield Φ_T ($\times 10^{-3}$)	0.001−1	4−10[b]	0.5−4
Off-state yield Φ_{off} ($\times 10^{-3}$)			0−0.5

[a] Number of on average detected photon counts at an average excitation energy of 500 W/cm^2. [b] The expected error is large because τ_T is in the same time range as the used sampling interval of 1 μs.

measured fluorescence intensity require different orientations of the transition moments with respect to the *z*-axis. Due to the used linearly polarized excitation conditions differences of the transition moments in *x*,*y*-plane and subsequent different excitation efficiencies control the fluorescence intensity distribution. Hence, the relation between fluorescence lifetime and intensity due to different orientations of the dipole moments is mostly smeared out in our data.

The broadness of the spectral distribution (Figure 4e) is not reflected in the lifetimes of the excited-states of the molecules, i.e., independent of the emission maximum, either blue or red shifted, the fluorescence lifetime and therefore the fluorescence quantum yield seems to be almost not influenced. This implies that fluorescence lifetime, and spectrum are independent characteristics of single molecules on glass surfaces. However, the oxazine derivative JA242 exhibits a slightly different behavior. With increasing emission maximum the fluorescence lifetime tends to decrease (Figure 4e).

On the other hand, dynamics in fluorescence intensity, spectrum and lifetime might be washed out using spot-integrated characteristics. To get information about temporal fluctuations, we positioned single JA242, JF9, and Cy5 molecules directly in the laser focus and monitored the fluorescence intensity, spectrum, and lifetime until irreversible photobleaching occurred. To minimize the probability of having two molecules simultaneously in the laser spot, suited molecules were selected from an image scan measured with reduced laser power. We studied the fluorescence characteristics of more than 200 individual molecules (90 Cy5, 70 JA242, and 70 JF9) adsorbed on glass at different excitation power. Since we were interested in fast fluctuations, the data was acquired in the time-tagged time-resolved (TTTR) mode, i.e. each photon count was registered by the macroscopic arrival time and the time lag with respect to the corresponding laser pulse. Binning into the desired time resolution was done after data acquisition.[39] At an excitation power of 500 W/cm^2 we detected on average ∼80000 photon counts for JF9 and JA242 molecules, whereas Cy5 molecules photobleached on average already after ∼30000 emitted photon counts (Table 2).

Fluctuations in Fluorescence Intensity Due to Intersystem Crossing. First we restrict our analysis and discussion to those time traces that showed typical fluctuations in fluorescence intensity without significant changes in fluorescence lifetime and spectrum (∼50% of all investigated molecules). In many cases it was easily possible to ascribe a measured fluorescence intensity time trace directly to one of the dyes due to the characteristic intensity fluctuations (compare Figure 5a, 5b, and 5c). Using a time resolution of 1 ms/bin, the intensity time traces of most JF9 molecules exhibit no off-states, whereas the oxazine dye JA242 tends to exhibit long off durations of up to seconds with a relatively small transition rate. In contrast, the carbocya-

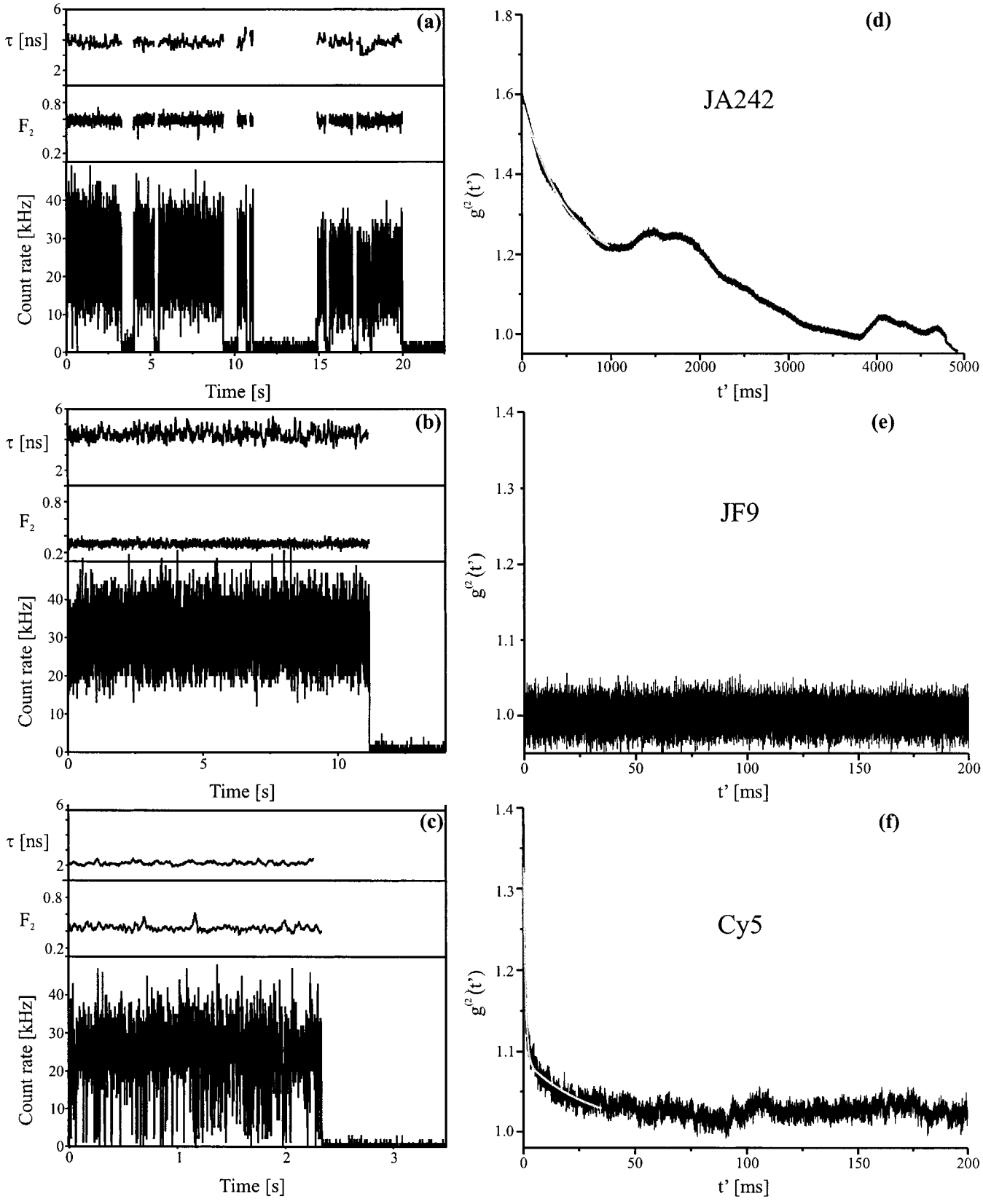

Figure 5. Analysis of single-molecule fluorescence intensity dynamics. Overall fluorescence intensity, fluorescence lifetime, and fractional intensity F_2 as a function of time for a single **(**a**)** JA242, **(**b**)** JF9, and **(**c**)** Cy5 molecule at an excitation power of 500 mW/cm^2. The fluorescence intensity and F_2 trace are plotted with a bin width of 1 ms. For fluorescence lifetime binning we applied a sliding-scale analysis using 500 subsequent photon counts. The corresponding calculated intensity autocorrelation functions for the **(**d**)** JA242, **(**e**)** JF9, and **(**f**)** Cy5 molecule, respectively, are plotted using a linear time axis. For intensity autocorrelation analysis we used a bin width of 10 μs for the JA242, 1 μs for the JF9, and 4 μs for the Cy5 intensity data, respectively. The first second of the autocorrelation function of the JA242 data is fit with a single exponential with a correlation time of $\tau = 488$ ms. The first few milliseconds of the Cy5 data reveal two correlation times of $\tau_1 = 880$ μs, $\tau_2 = 31$ ms.

nine dye Cy5 shows predominantly faster blinking with a higher transition rate.

In addition, it should be mentioned that our measurements have been performed under ambient conditions (room temperature, air) where direct observation of intersystem crossing is extremely difficult due to short triplet lifetimes (collisional quenching by oxygen) as well as rapid photobleaching. Therefore most single-molecule triplet studies have been performed at cryogenic temperatures[34,35,55] or under vacuum conditions.[29,30] In air-saturated ensemble solutions, the triplet state lifetimes τ_T of rhodamine, oxazine, and carbocyanine dyes vary between less than 1 μs up to several μs with intersystem crossing rates k_{ISC} from 4.2×10^5 to 2.8×10^7 s^{-1}.[50,56−58] In vacuum, Weston et al.[29] found triplet lifetimes of 4−100 ms for single $DiIC_{12}$ molecules (a carbocyanine derivative) with a triplet yield of 4×10^{-4}. In accordance with these results, English et al.[30] found triplet lifetimes of ~100 ms at reduced pressure with yields of 3.5×10^{-4} for the same chromophore immobilized in thin polymer films. As obvious as they are from the fluorescence time traces shown in Figure 5, we found off times in the same time range for most oxazine and carbocyanine dyes under air-equilibrated conditions.

However, contrary to the oxazine and carbocyanine intensity traces, most intensity traces of JF9 molecules show no intensity fluctuations on a 1 ms time scale (Figure 5). To quantitatively analyze the intensity fluctuations, we employed the second order intensity autocorrelation method previously used to analyze fluorescence intensity fluctuations of single molecules at cryogenic temperatures,[60] and more recently at room temperature.[24−26] The normalized intensity autocorrelation function is defined as the probability of detecting pairs of photons separated in time by an interval t' (eq 2).

$$g^{(2)}(t') = \frac{\langle I(t)I(t+t')\rangle}{\langle I(t)\rangle^2} = \frac{\langle N(t)N(t+t')\rangle}{\langle N(t)\rangle^2} \qquad (2)$$

I(t) is the fluorescence intensity measured in the integration interval (bin time) centered at time *t*, *N(t)* is the number of photon counts detected in the same interval, and $\langle N(t)\rangle^2$ is the square of the mean intensity detected per bin time. Examples of $g^{(2)}(t')$ calculated from the data of Figure 5a−c with a bin width of 10, 1, and 4 μs, respectively, are shown in Figure 5d−5f. For correlated events the intensity autocorrelation function exhibits values >1. As already indicated by the relatively homogeneous fluorescence intensity trace (Figure 5b), the intensity autocorrelation functions obtained from different JF9 molecules reveal no correlation term at an excitation energy of 500 W/cm^2 (Figure 5e).

To investigate the influence of the excitation energy on the probability to resolve short-lived triplet states from fluorescence fluctuations we calculated the rate constants $k_{0,1}$ for excitation from the electronic ground-state S_0 to the first excited-state S_1 from the average laser power, I (W/cm^2), and the absorption cross section $\sigma_{0,1}(\lambda)$ (cm^2), at the wavelength λ using eq 3:

$$k_{0,1}(\lambda) = I\sigma_{0,1}(\lambda)\gamma \qquad (3)$$

where $\gamma = \lambda/hc$ (h is the Plank constant and c the velocity of light in a vacuum). With an absorption cross section of $\sim 10^{-16}$ cm^2 at 635 nm[48,58] and an average laser power of 500 W/cm^2 a JF9 molecule will be excited with a rate $k_{0,1}$ of $\sim 1.6 \times 10^5$ s^{-1}. Here we have to point out, that the exact location of a molecule in the output laser beam was a priori not known and since the polarization was not controlled, the absolute excitation energy is not well defined in the applied experimental setup. Hence, on average lower excitation rates will result. With a fluorescence quantum yield Φ_f of ~0.90 and an overall detection efficiency of 0.10 at the glass/air interface[22,28] a fluorescence intensity of 14.4 kHz should be detected. This value is considerably smaller than the intensity recorded from the JF9 molecule shown in Figure 5b, but comparable to the average fluorescence intensity detected from single JF9 molecules at an excitation power of 500 W/cm^2. Comparison of typical triplet lifetimes of rhodamine derivatives[57,58] ($\tau_T = 4-6$ μs) and the average time-lag between subsequent photon counts of ~70 μs (count rate of 14.4 kHz) points out that the triplet term cannot be resolved using low excitation energies. Therefore, we decided to use an excitation energy of 5 kW/cm^2 in the following experiments. On the other hand, it is considerably more difficult to detect enough photon counts from single molecules for statistical analysis under air-equilibrated conditions. Especially the carbocyanine dye Cy5 photobleached on an average already in less than 500 ms using an excitation energy of 5 kW/cm^2. Hence, we decided to increase the size of the pinhole (200 μm) and lower the excitation power to 2 kW/cm^2 for Cy5 experiments.

Comparison of the fluorescence fluctuations recorded from the three different chromophores under lower and higher excitation energies (compare Figure 5 with Figure 6) indicates that the principle fluorescence characteristics of the molecules are unchanged. The rhodamine derivative exhibits the highest count rates of up to 500 kHz. However, upon binning of the data into shorter time bins (typically 1 μs) an correlation term $g^{(2)}(t') > 1$ appears in the corresponding autocorrelation function (Figure 6e). The resulting intensity autocorrelation functions were fitted by an exponential model (eq 4),

$$g^{(2)}(t') = 1 + \sum_{i=1}^{n} A_i e^{-t'/\tau_{ac}{}^i} \qquad (4)$$

where $\tau_{ac}{}^i$ denotes the time constant, and A_i the amplitude of the ith component. It has to be considered that an intensity autocorrelation analysis alone without spectral and time-resolved data leads to very little information on the nature of the underlying dynamics. However, here we used $g^{(2)}(t')$ only as a method to directly determine the time constants of the off-states and their corresponding amplitudes from fluorescence intensity traces that show no apparent evidence of spectral diffusion or variations in other photodynamic parameters. Under the assumptions that the autocorrelation is only examined at times that are large compared to the fluorescence lifetime of the molecule and that the integration times are smaller than the average on- and off-times, τ_{ac} of the ith component can be expressed as[26,59]

$$\frac{1}{\tau_{ac}} = \frac{1}{\tau_{off}} + \frac{1}{\tau_{on}} \qquad (5)$$

$$A \cong \frac{\tau_{off}}{\tau_{on}} \qquad (6)$$

With these equations the off-time can be estimated by $\tau_{off} = (1 + A)\tau_{ac}$. As can be seen in Figure 6a−f, the preexponential term A is larger for a molecule which spends more time in the off-state. The transition yield of the off-state Φ_{off} can be roughly estimated from the on-time τ_{on}, the detected count rate I_{det}, the fluorescence quantum yield Φ_f, and the detection efficiency Φ_{det} of 0.05 at each detector (eq 7).

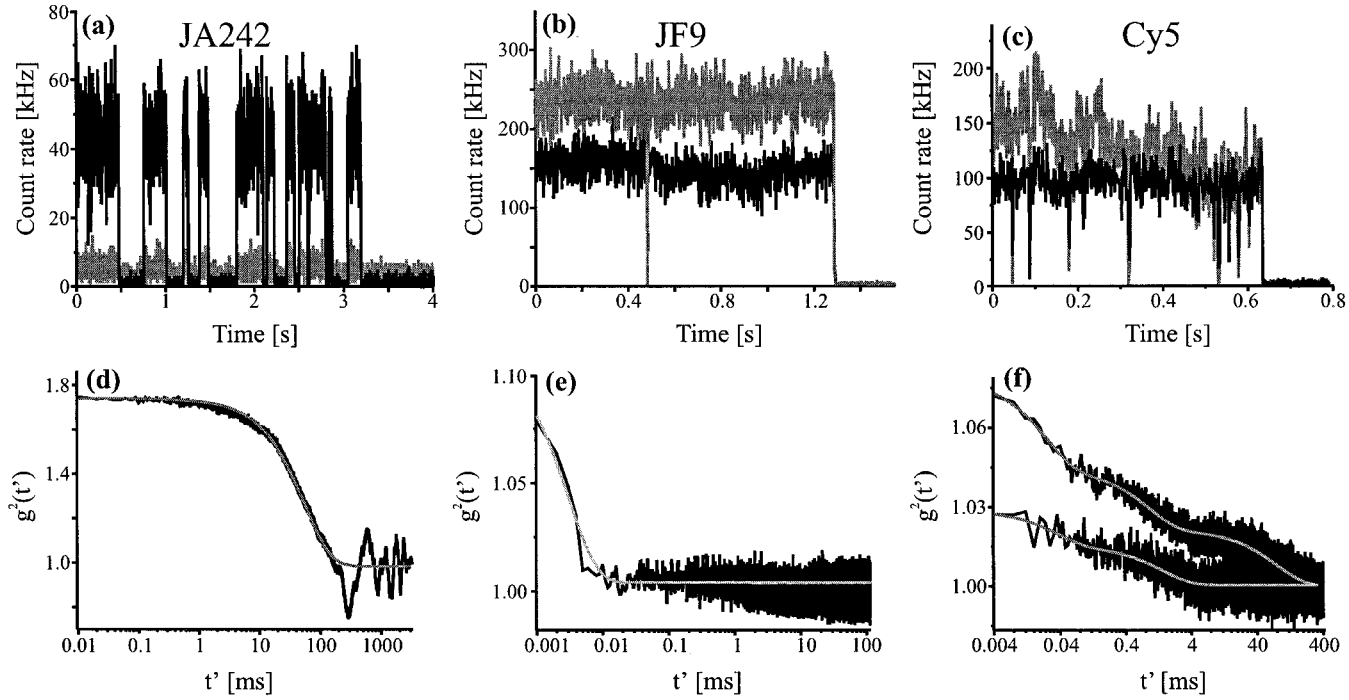

Figure 6. Fluorescence intensity recorded from single molecules at detector 1 (gray) and detector 2 (black) versus log time for **(**a**)** a JA242, **(**b**)** a JF9 at an excitation of 5 kW/cm^2, and **(**c**)** a Cy5 molecule at an excitation energy of 2 kW/cm^2. The data are binned into 1 ms time bins. The corresponding intensity autocorrelation were calculated from the intensity data recorded at detector 2 using a time-resolution of 10 μs for the JA242 data **(**d**)**, and a time-resolution of 1 μs for the JF9 data **(e)**. For the Cy5 molecule the intensities recorded at both detectors binned into 4 μs time bins were used separately for the construction of the corresponding autocorrelation functions **(**f**)**.

$$\Phi_{off} = \frac{\Phi_f \Phi_{det}}{\tau_{on} I_{det}} \tag{7}$$

If we ascribe the measured off-states to transitions into short-lived triplet states a single-exponential fit revealed a triplet lifetime τ_T of 3.5 μs with an intersystem crossing rate k_{ISC} of 1.5×10^6 s^{-1} (corresponding to a triplet yield Φ_T of 6×10^{-3}) for the JF9 molecule (Figure 6b,e). This values are similar to triplet parameters of red-absorbing rhodamine derivatives obtained from ensemble measurements in solution.[58] Nevertheless, a τ_T of 3.5 μs appears to be the shortest triplet lifetime ever recorded from single-molecule fluorescence intensity time traces of rhodamines on surfaces at room temperature. Here it must be considered that eqs 4 and 5 hold only for integration times smaller than the off times. Hence, the error expected in the short-lived triplet state of JF9 is large because τ_T is in the same time range as the used sampling interval of 1 μs.

In addition, only a rough estimate of the width of distribution of the triplet parameters can be given because only a limited number of JF9 molecules (only 3 out of 20 molecules) were found that exhibited sufficient photon count statistics to resolve triplet states in the range of a few μs. However, for these JF9 molecules, the obtained distribution in triplet parameters appears to be rather narrow with τ_T varying between 2 and 7 μs and intersystem crossing yields Φ_T ranging from 4×10^{-3} to 1×10^{-2} (Table 2).

As expected for triplet states the fluorescence intensity traces of single oxazine molecules (JA242) exhibit relatively long off-times (Figure 6a), independent of the excitation energy (0.5−5 kW/cm^2). The autocorrelation analysis of the data shown in Figure 6a reveals a triplet lifetime τ_T of 98 ms with a relatively low intersystem crossing rate of 1.3×10^3 s^{-1} ($\Phi_T \sim 5 \times 10^{-6}$). On the other hand, the intersystem crossing rate should increase with increasing excitation energy and by comparing the intensity data shown in Figures 5a and 6a one might recognize that in fact an increase in k_{ISC} at higher laser energy is obvious. In addition, it has been shown,[60] that the triplet lifetime of adsorbed oxazine molecules increases considerably, e.g., the triplet lifetime τ_T of oxazine adsorbed on cellulose was measured to 4.3 ms which is ∼300 times longer than that in solution. However, due to the broad distribution of triplet parameters obtained from single molecule experiments under various conditions (N_2, O_2) and unsatisfying photon statistics (due to rapid photobleaching and low transition yields) a clear-cut assignment of such long off periods to triplet states is difficult. For example, even under oxygen saturated conditions, we found strong variations in triplet lifetimes comparable to the values obtained under air-equilibrated conditions between 1 and 150 ms with triplet yields ranging from 10^{-6} to 10^{-3} for individual JA242 molecules. The reason for this strong discrepancy in triplet characteristics between the rhodamine and the oxazine derivative is not yet understood and will be subject of further investigations.

While all autocorrelation functions for JF9 and JA242 could be well fit by a monoexponential function, the situation is more complex for the carbocyanine dye Cy5 (Figure 6c,f). In most cases the intensity autocorrelation function of single Cy 5 molecules had to be described by a biexponential model. In Figure 6f the intensity autocorrelation functions recorded with both detectors are shown. While $g^{(2)}(t')$ of channel 2 exhibits two decay times, the data recorded on channel 1 required a third component to account for slow spectral diffusion of the molecule in the ms to s time range. Typical values obtained for Cy5 molecules are $\tau_{1off} = 55$ μs with a transition yield $\Phi_1 = 2 \times 10^{-3}$ for the short component and $\tau_{2off} = 2$ ms with a transition yield $\Phi_2 = 2 \times 10^{-4}$. In accordance with Veermann et al.,[28] we attribute the shorter component which also shows a considerable distribution of ∼10−150 μs to the triplet lifetime of the carbocyanine dye Cy5, whereas the longer component of 0.5−5 ms might arise from conformational fluctuations in

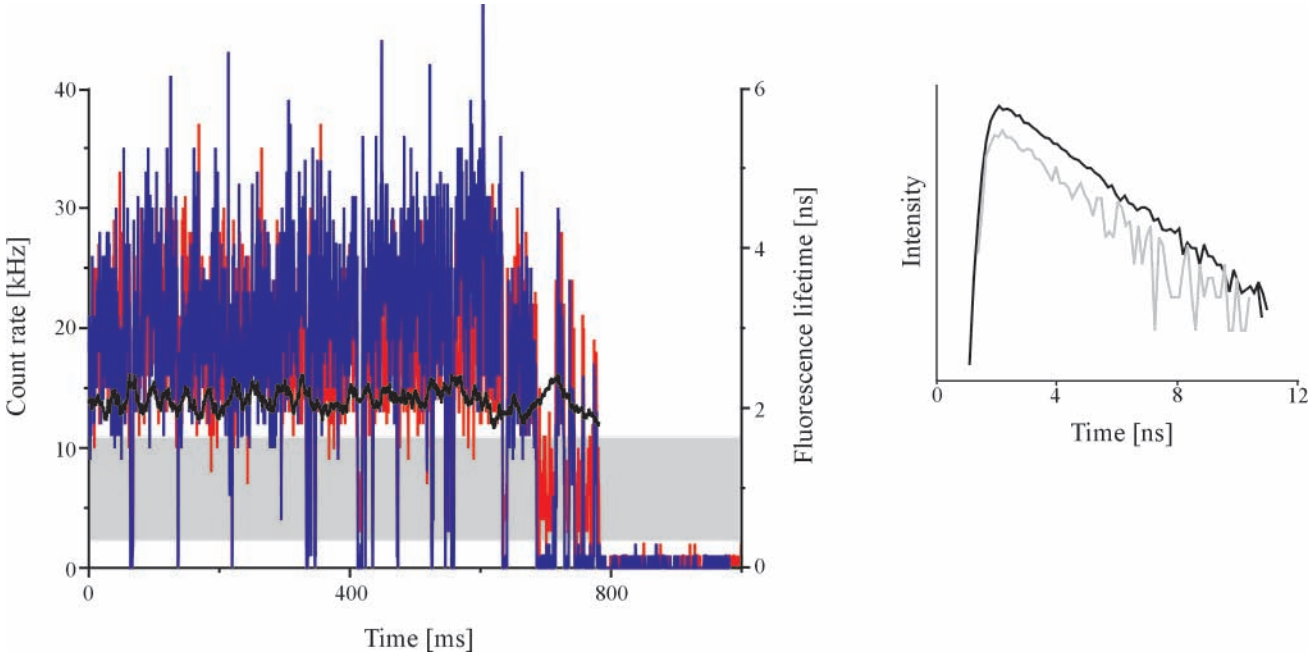

Figure 7. Fluorescence intensity time trace (1 ms/bin) and fluorescence lifetime measured at both detectors (Blue: intensity detector 1. Red: intensity detector 2. Black: fluorescence lifetime.) from a single Cy5 molecule at an excitation energy of 2 kW/cm^2. In addition, the fluorescence decays revealed from an intensity classification are shown. The gray marked decay corresponds to the dim-state with a fluorescence intensity of 2−11 kHz, whereas the black decay shows the photon counts from the on-state (>11 kHz). Both decay can be described satisfactorily with a single-exponential model with a decay time of $\tau \sim 2$ ns.

the polymethine backbone, such as cis/trans isomerization or small distortions of symmetry or planarity of the chromophore leading to non- or only weakly absorbing and fluorescing states. Experiments probing the dependence of the fluctuations on excitation energy showed little evidence for light-induced processes. Table 2 summarizes the triplet parameters obtained from single JA242, JF9, and Cy5 molecules.

Fluctuations in Fluorescence Lifetime and Spectrum. Spectral diffusion of sulforhodamine,[21,24] and carbocyanine dyes[26] have been studied already extensively by spectrally resolved single-molecule spectroscopy. The experimental data showed that spectral diffusion occurs over a broad distribution of time scale (from milliseconds to seconds) and amplitude. In general, these fluctuations in emission spectra have been attributed to transitions between different potential minima of the molecule's energy landscape. These transitions might be due to either conformational changes of the backbone or side chains of the molecule (intramolecular motion) or small motions of the microscopic environment and subsequent distortion of the chromophore (intermolecular motion). It is obvious that any conformational change accompanied by a distortion of the backbone of the chromophore should result in a changed absorption cross section at the excitation wavelength, a shift in the absorption and emission maxima and a changed radiative decay rate and emission yield of the chromophore.[24−26] Hence, monitoring of the fluorescence lifetime with high temporal resolution should allow to directly follow conformational transitions in the chromophore. Moreover, the simultaneous time-resolved pursuit of the excited state kinetics and emission maximum reveals an elegant method to answer the question whether a change in emission spectrum is accompanied by a change in emission yield. However, since the molecule is resident in each state partly only for a time of the order of milliseconds, it is difficult to acquire a fluorescence decay with sufficient photon count statistics for an unequivocal determination of the decay rate. Therefore, we monitored the fluorescence emission maximum and lifetime of the chromophore simultaneously applying the time-tagged time-resolved (TTTR) mode. In combination with a sliding-scale analysis (see Experimental Section) fast fluctuations in fluorescence lifetime can be resolved even in the millisecond range.[43]

Approximately 20% of all molecules investigated in this study showed clear evidence of spectral diffusion or changes in fluorescence lifetime. The other molecules exhibited more or less pronounced rotational fluctuations,[61] i.e., sudden changes in fluorescence intensity with unchanged emission spectrum and lifetime. Although we observed a wide variety of fluctuations for the investigated dyes we focus first on the carbocyanine dye Cy5 and the two independent off-states observed by intensity autocorrelation analysis. If we have a closer look at some fluorescence intensity time traces of Cy5 molecules, often two discrete intensity levels are obvious. Surprisingly, some of these molecules did not enter a real off-state, i.e., the count rate did not drop to the background level, but instead exhibited a certain fluorescence intensity (Figure 7). In addition, in most cases these dim-states exhibited a red-shifted emission maximum.

The extent of fluorescence intensity change and spectral diffusion varies significantly from molecule to molecule. However, because the intensity fluctuations take place in the same time domain as the second off-time revealed from the autocorrelation analysis we assume that the observed off-states of 0.5−5 ms and dim-states have the same origin. For example, if we consider only the shorter wavelength channel (blue channel) of the Cy5 molecule in Figure 7 we have to conclude that the molecule entered a real off-state state while the other detector (red channel) still recorded a distinct intensity (see Figure 7 at ∼400 ms and after ∼700 ms). In addition, a change in transition probability between the on- and dim-state occurred at ∼700 ms. With the knowledge of the detection sensitivity at different wavelengths (Figure 3) we calculated an emission maximum for the dim-state of >700 nm. On one hand, above 700 nm the detection sensitivity is at most one-third of the detection sensitivity at the wavelength of the on-state (∼670

nm). In accordance with this, the overall count rate obtained during the dim-state is about only one-fifth of the count rate obtained during the on-state. On the other hand, the fluorescence lifetime remains more or less unchanged at ~2 ns over the whole time trace independent of spectral diffusion. However, the fluorescence lifetime trace shown in Figure 7 has been calculated by adding up 500 subsequent photon counts disregarding the time lag (the intensity information). To directly compare the fluorescence lifetimes of the levels which exhibited higher and lower fluorescence intensity, we used an intensity classification. By this, all photon counts from channels which contained more than 11 counts/ms (defined as on-state) were fed into one histogram of arrival times while the photon counts from channels with 2−11 counts/ms (defined as dim-state, gray area in Figure 7) were fed into another histogram. This procedure yielded two fluorescence decays which could both be well described by the same single-exponential fit with a decay time of ~2 ns (Figure 7). Hence, the fluorescence lifetime of the ordinary on-state and the red-shifted dim-state are identical within experimental error.

Out of the three dyes investigated, these characteristics, i.e., fast spectral fluctuations in the millisecond range, were only found for the carbocyanine derivative Cy5. We assume that dependent on the extent of the spectral jumps off-states are detected. The unchanged radiative lifetime is surprising, since we attributed the slower fluctuations observed in the ms time range (0.5−5 ms) to a kind of twist around the polymethine backbone which should be accompanied by a changed emission yield and radiative decay rate. This implies that the observed spectrally shifted dim-states are obviously not due to a kind of distortion of the chromophores backbone. Such a distortion should significantly alter the radiative lifetime owing to a delocalization of electron density and greater access to nonradiative decay channels.

Furthermore, comparison of intensity time traces recorded from different Cy5 molecules implies that the reduced photostability is connected with the off- or dim-state. Cy5 molecules which showed a higher transition probability photobleached more often after less than 1 s at an average excitation energy of 2 kW/cm^2. As can also be seen in Figure 7, the Cy5 molecule photobleached in the dim-state.

In the following, we stress on certain new aspects which can be investigated by the applied multiparameter detection. Figure 8 shows five time-resolved traces of the fluorescence intensity, lifetime, and fractional intensity F_2 of single rhodamine dyes JF9 (Figure 8a,e), and oxazine dyes (Figures 8b-8d) at different excitation energies. The JF9 molecule shown in Figure 8a exhibited an almost constant fluorescence intensity and lifetime (~4 ns) with a kind of time dependent red shift of the emission maximum from 665 to 670 nm during the first 2 s. During this time the molecule jumped two times to a state with blue shifted emission maximum (~655 nm). After ~2.5 s the JF9 molecule finally decided to stay in the blue shifted state until irreversible photobleaching occurred.

Interestingly, the fluorescence lifetime of this JF9 molecule (Figure 8a) remains almost unchanged with, if at all, only a very slight increase in fluorescence lifetime after the dramatic change in fractional intensity F_2 occurred. Moreover the fluorescence intensity was constant before and after the spectral jump. This behavior is always surprising since the apparatus exhibits a different detection sensitivity for each wavelength and therefore changes in the emission wavelength should always be connected with a changed count rate. In the case of the JF9 molecule in Figure 8a, a higher count rate should be detected after the spectral jump to ~655 nm. However, either the emission yield dropped after the spectral jump (which is unlikely due to the unchanged fluorescence lifetime) or, more likely, our model which assumes a constant Stokes shift and unchanged shape of the absorption and emission spectra can no longer be maintained. The intensity fluctuations that occurred during the last ~500 ms are most probably due to a change in the orientation of the transition dipole.

The time trace of the molecule portrayed in Figure 8b was obtained from a single JA242 that showed a hypsochromic spectral jump after about 700 ms while the fluorescence lifetime remained unaffected. In addition, other photophysical parameters changed simultaneously, i.e., in the state with the red-shifted emission maximum (first 700 ms) the molecule showed no intensity fluctuations indicating a very low intersystem crossing rate while after the transition to the blue-shifted state relatively fast blinking in the order of milliseconds was observed.

Interestingly, the spectral jump occurred "during" an off-state (as indicated by the spike in the F_2-graph), i.e. the molecule jumped into an off-state and after 25 ms it recovered now exhibiting altered physical properties such as blue-shifted emission maximum and increased intersystem crossing rate. It is found quite often for all classes of dyes that significant spectral jumps occurred during off-states. In addition, the count rate of the JA242 molecule is considerably lower after the spectral jump although a higher count rate would be expected due to the higher detection sensitivity at an F_2-value of 0.78 compared to 0.89 before the spectral jump (for comparison see Figure 3c−f). From Figure 8a,b we have to conclude that, with exception of the radiative lifetime, some chromophores suddenly completely change their photophysical properties. Here one has to keep in mind, that our interpretation of the fractional intensity in terms of emission maxima holds only true if we assume an unchanged shape of the absorption and emission spectra, and a constant Stokes shift of 20 nm. Recently,[26] Weston et al. could demonstrate, that the emission spectra of single $DiIC_{12}$ molecules exhibited a wide distribution of shape. While some spectra showed narrow well resolved bands implying that the molecule is coupled to a smaller number of vibrations than the average molecule, other molecules appeared to couple to a larger number of vibrations resulting in a broad unresolved emission spectrum. Spectral shifts far from the average have been attributed to differences in the binding site of the molecule, quite possibly due to electrostatic interactions between the charged chromophores and the glass surface.

Thus, the observed changes in emission yield might result from smaller or larger changes in the absorption and emission shape leading to a lower absorption cross section at the excitation wavelength or changed transmission intensities with respect to the filter system. Hence, the calculated F_2-value might change drastically. If for example some vibrational states of the chromophore are blocked it is also likely that the radiative and nonradiative rates change. However, our data clearly demonstrate, that some chromophores jump to other potential minima on their landscape with almost no change in radiative decay rate.

On the other hand, independent of the chromophore structure, we found only a few single molecules that showed both, changes in spectrum and radiative decay rate. The JA242 molecule shown in Figure 8c exhibited a spectral jump after about 12 s from an emission maximum at ~680 to ~640 nm. Not simultaneously, but instead about 50 ms later, the fluorescence lifetime increased from ~2.5 to ~4 ns accompanied by a change in the blinking frequency. Here the longer lifetime and lower overall fluorescence intensity are in accordance with the

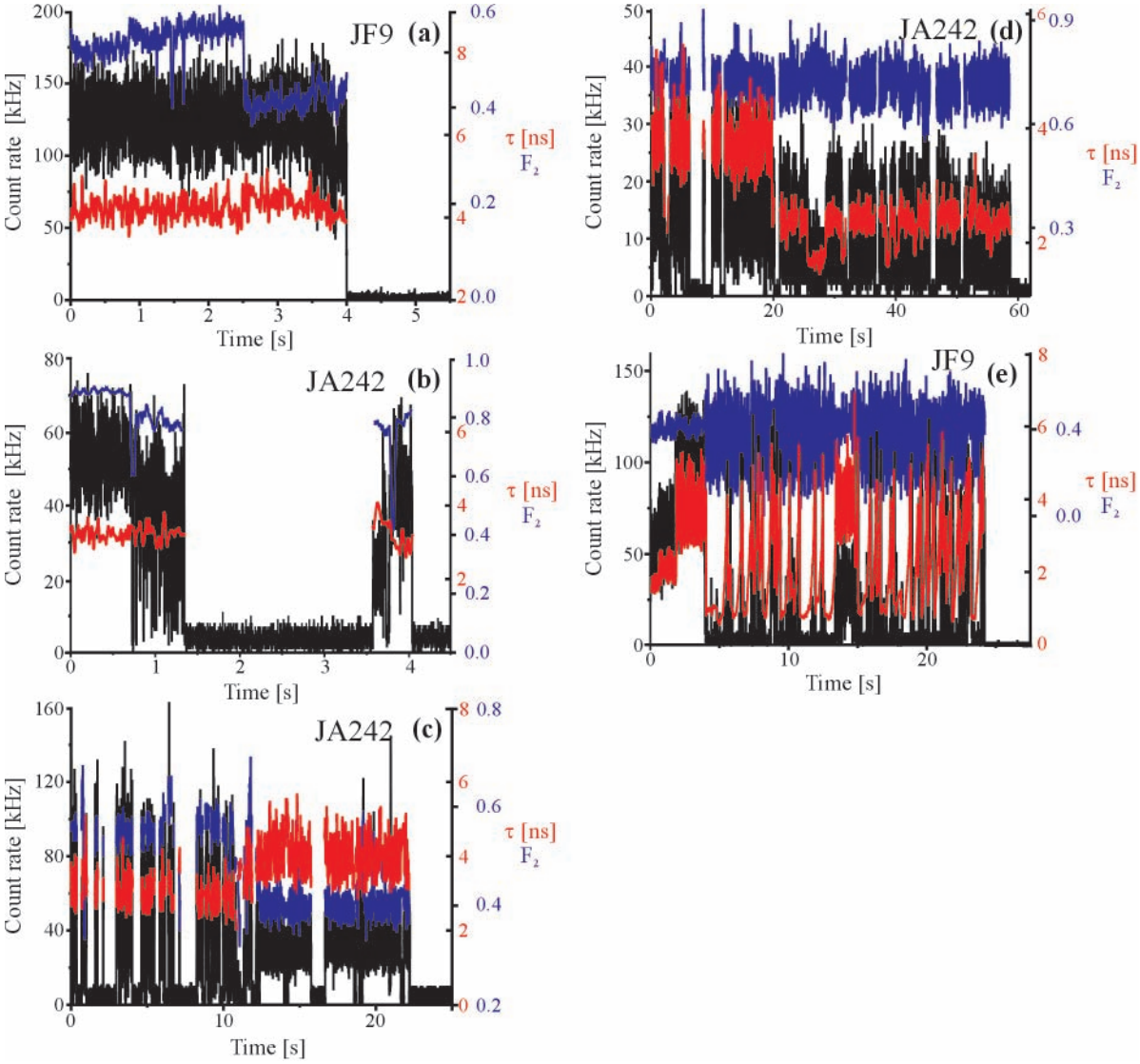

Figure 8. Analysis of single-molecule photophysical dynamics. Overall fluorescence intensity (black), fluorescence lifetime (red), and fractional intensity F_2 (blue) as a function of time for single JF9 and JA242 molecules at different excitation power. **(a)** JF9 at 5 kW/cm^2, **(b)** JA242 at 1 kW/cm^2, **(c)** JA242 at 5 kW/cm^2, **(d)** JA242 at 1 kW/cm^2, and **(e)** JF9 at 1 kW/cm^2. The fluorescence intensity and fractional intensity recorded at detector 2 F_2 are plotted with a bin width of 1 ms. For clarity of presentation, the shown F_2-values are averaged over 10 data points. For fluorescence lifetime binning we applied a sliding-scale analysis using 500 subsequent photon counts. Variations in the background level are due to the different excitation energies and plotted maximum count rates.

detection sensitivity of the setup. Although the fluorescence quantum yield in the blue-shifted state is obviously higher, the recorded count rate dropped due to the reduced detection sensitivity at 640 nm.

We also observed molecules exhibiting distinct changes in fluorescence lifetime that can clearly be distinguished from variations due to shot-noise. Especially, oxazine molecules exhibited a high sensitivity for changes in the radiative decay rate (about 30% of all molecules investigated) while lifetime variations are rather rare for the other types of dyes (10% for JF9, and 13% for Cy5, respectively). About 50% of those molecules showed a direct correlation between fluorescence lifetime and fluorescence intensity, i.e., states with a relatively long lifetime showed an adequately higher fluorescence intensity. Two examples of this class of molecules are portrayed in Figure 8d (JA242) and Figure 8e (JF9).

The JA242 molecule exhibited three discrete on-states with distinct fluorescence lifetimes of 3.9, 2.2, and 1.6 ns, respectively, and an additional off-state. Surprisingly, only the fluorescence lifetime and fluorescence intensity changed. The molecule did neither exhibit a varying intersystem crossing rate in any of the states nor did the length of the off-states obviously change and finally it did not show any dramatic changes in the emission spectrum.

The JF9 molecule shown in Figure 8e exhibited similar photophysical dynamics. It showed relatively fast changes between three states with different fluorescence yield and lifetime. Comparison with the count rate after irreversible photobleaching occurred (~24 s) implies that the states with very low count rate are dim-states with unchanged spectral characteristics but well distinct radiative decay rate, e.g., as expected from a bimolecular quenching mechanism. Since the sliding-scale analysis averages over 500 subsequent photon counts, we decided to sum up all photon counts obviously belonging to different fluorescence intensity and lifetime states manually. If we would have used a simple intensity classification, the different radiative decay times of the state at the beginning (0−2 s) and at around 14 s would have been attached to the same state. Figure 9 shows the resulting three decay curves which could all be well described by single exponential

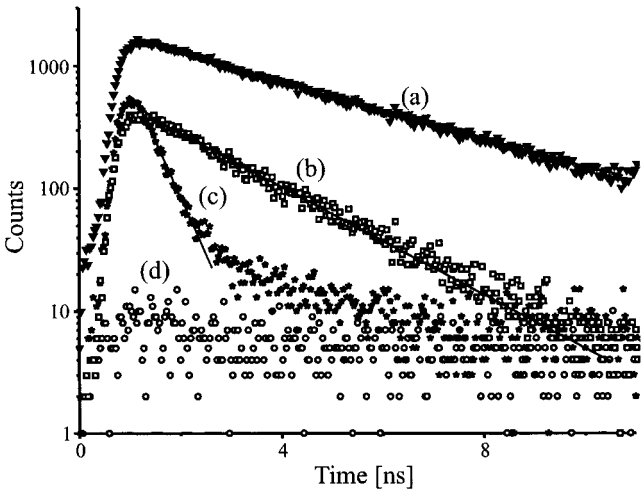

Figure 9. Fluorescence decays of different intensity levels of the JF9 molecule shown in Figure 8e. **(a)** The high-intensity state with a decay time of 3.83 ns, **(**b**)** the medium-intensity state with a decay time of 1.98 ns, and **(**c**)** the low-intensity level with a decay time of 0.55 ns. In addition, the decay of the background recorded during 10 s after the molecule photobleached is shown.

models: (a) the high-intensity state with a decay time of 3.83 ns, (b) the medium-intensity state with a decay time of 1.98 ns, and (c) the low-intensity level with a decay time of 0.55 ns. In addition to the fluorescence decays of these three states the decay of the background recorded during 10 s after the molecule photobleached, is shown in Figure 9. For construction of the decays only the photon counts detected at the longer-wavelength detector (detector 2) were taken into account as for this wavelength window the background is somewhat lower (almost no scattered light). As can be clearly seen in Figure 9, the background signal did not contribute significantly to the measured signal, i.e., the low background intensity allowed the definite identification of a dim-state with a fluorescence lifetime of 0.55 ns and low emission yield, but unchanged emission maximum.

To demonstrate that these molecules exhibited a constant emission maximum over the whole time trace, we used autocorrelation analysis of the measured F_2-values. As expected, no correlations were found in the autocorrelation function of the F_2-values (data not shown). However, one has to be cautious with autocorrelation analysis of F_2-values as they are not always expressive for spectral variations: Off-states also exhibit a certain F_2-value given by the background count rates at each detector. Hence, the F_2-autocorrelation analysis would yield the same correlation terms as the intensity autocorrelations. The same holds true for fluctuations in fluorescence lifetime and has to be kept in mind for autocorrelation analysis of these parameters.

Before discussing the changes in radiative decay time, we want to focus on changes in emission maximum, i.e., spectral diffusion of the chromophore. And even more important on the fact, that most observed spectral fluctuations were not accompanied by fluctuations in radiative lifetime.

In principle, there are several mechanisms which trigger spectral fluctuations: isomerization or distortion of the chromophores backbone or side chains (generally conformational transitions),[21,24,25] changes in vibrational states,[26] contact ion pair formation of the positively charged basic chromophores,[27] and changes in electron density at certain atoms in the chromophore in either the ground-state or first excited singlet state by internal or external electron donating or accepting groups,[62] i.e., changes in the HOMO and LUMO energies.[48,49,63] Distortions of the chromophore backbone are very likely to be always accompanied by changes in the radiative decay rate. However, on the other hand, it is known that contact ion pair formation, conformational changes in side chains, inhibition of vibrations, and changes in the electronic levels of the chromophore do not automatically influence the excited-state kinetics to the same extent as they change the absorption and emission maxima.

The influence of changes in the electron density at certain atoms in the chromophore can be exemplified for the rhodamine derivative JF9. The pentafluorophenyl group connected to the central carbon atom of the chromophore exhibits an important influence on the absorption and emission maximum of the chromophore. Due to its electron accepting properties, the LUMO of the chromophore decreases thereby shifting the absorption and emission maximum toward longer wavelengths. It follows from AM1 calculations that in the ground-state S_0 the plane of the phenyl substituent is held nearly perpendicular to the xanthene moiety in rhodamines with bulky phenyl substituents in ortho-position. Hence, in rhodamines with steric pretentious substituents in the ortho-position of the phenyl ring, the fluorescence lifetime of the chromophore is only marginally influenced by the substituents at the phenyl ring.[63] Thus, with respect to the interaction geometry, counterions, impurities, or the surface groups ($-NH_2$, $-OH$) themselves may influence the electron density at atoms of the chromophore thereby changing the absorption and emission maximum. Of course, it cannot be excluded that such interactions also significantly influence the excited state kinetics. However, it is unlikely that they are responsible for the observed rapid fluctuations in fluorescence lifetime which could all be well described by single-exponential decays. The fact that all other photophysical properties such as transition rates into off-states and emission spectrum are not altered gives evidence for an external bimolecular quenching mechanism. At present the source of the external quenching (whether impurities or surface groups) remains subject of speculation. Nevertheless, the existence of discrete fluorescence intensity states in combination with various distinct fluorescence lifetimes supports the idea that certain reaction geometries are required. Dependent on the interaction geometry different quenching efficiencies and mechanisms may result.

For simplification we tend to divide the observed photophysical dynamics into three subclasses: (a) molecules which show dynamic changes in emission spectrum accompanied by changes in transition rates into off- or dim-states, and changes in radiative decay rate, (b) molecules exhibiting dynamic changes in emission spectrum, but a constant radiative decay rate, and (c) molecules revealing only dynamic changes in radiative decay rate. However, we have to point out, that in general any change in nuclear coordinates or excited state levels of the chromophore either induced externally or internally influences all photophysical parameters. Hence, the experimentally derived classification might be rather controlled by several theoretical considerations:

First, various transitions of the molecule on the potential energy landscape or various interactions with electron donating or accepting groups will change each photophysical parameter to a different extent. Due to the low photon count statistics obtained from single molecules minor dynamic changes are hardly resolved. In addition, especially in periods showing fast fluctuations, changes in transition probabilities might be washed-out. Second, surface inhomogeneity has to be taken into account,

i.e. each parameter might be more or less influenced dependent on surface preparation, and the relative position and orientation of the chromophore on the surface. Third, in all single-molecule studies two kinds of selection of suited molecules occur: (a) only molecules which can be monitored over a certain time can be selected and discussed and (b) the selection of suited single-molecule data always underlies a subjective choice.

Conclusions

We have demonstrated that spectrally resolved fluorescence lifetime imaging microscopy (SFLIM) at the single-molecule level is a new powerful technique for classification and quantification of photophysical parameters. The combination of high sensitivity and multiparameter detection enabled us to uncover the inhomogeneity of photophysical properties of single molecules. Therefore, it is ideally suited to monitor the local environment around probe molecules, e.g., in living cells or as a contrast giving method in high precision distance measurements.[51,52]

Spectrally- and time-resolved detection of rhodamine, oxazine, and carbocyanine molecules on a glass surface indicates a wide variety of photophysical dynamics. All three chromophores exhibit fast fluctuations in fluorescence intensity which we attribute to intersystem crossing into short-lived triplet states. The triplet lifetime of the rhodamine derivative JF9 was found to be remarkable short compared to the oxazine dye. For the carbocyanine derivative Cy5 an additional transition into a real off- or red-shifted dim-state with a lifetime in the millisecond range was determined. Surprisingly, the red-shifted dim-state exhibits the same radiative decay rate of ~2 ns as the regular on-state. About 50% of all molecules independent of the chromophore structure showed neither significant fluctuations in emission spectrum nor in fluorescence lifetime under different excitation energies. It still remains open for further investigations whether the variations in photophysical parameters are due to inhomogeneous environmental distributions or insufficient sampling time due to rapid photobleaching (especially for Cy5 molecules).[28]

Furthermore, our observations imply that under air-equilibrated conditions (1) about 20% of all molecules (JA242, JF9, Cy5) show significant spectral fluctuations, (2) more than 70% of all spectral jumps are not accompanied by changes in fluorescence lifetime, (3) spectral jumps often occur during off-states, (4) some molecules (5−15% of all molecules) exhibit fluctuations in fluorescence lifetime directly correlated to intensity, (5) the molecules which show direct correlation between fluorescence lifetime and count rate do not show significant alterations in emission maximum and triplet parameters, and (6) the described characteristics appear to be not light-induced and are not restricted to one class of chromophores, but instead, they are a general feature of all classes of dyes investigated in this study. Finally, one should consider that the photophysical characteristics of single molecules might be influenced by a large stochastic component due to various contributions from environmental factors. Hence, a complete explanation of all experimental data with high confidence is very difficult to achieve.

Acknowledgment. The authors thank J. Wolfrum and K. H. Drexhage for fruitful cooperation and stimulating discussion. K. H. Drexhage and J. Arden-Jacob for the generous disposal of the oxazine derivative JA242 and the rhodamine derivative JF9. J. Enderlein for help in theoretical considerations. Financial support by the Volkswagen-Stiftung (Grant I/74 443) and the Bundesministerium für Bildung, Wissenschaft, Forschung und Technologie (Grant 11864 BFA082) is gratefully acknowledged.

References and Notes

(1) Betzig, E.; Chichester, R. J. *Science* **1993**, *262*, 1422.
(2) Ambrose, W. P.; Goodwin, P. M.; Martin, J. C.; Keller, R. A. *Science* **1994**, *265*, 364.
(3) Trautman, J. K.; Macklin, J. J.; Brus, L. E.; Betzig, E. *Nature* (*London*) **1994**, *369*, 40.
(4) Xie, X. S.; Dunn, R. C. *Science* **1994**, *265*, 361.
(5) Macklin, J. J.; Trautman, J. K.; Harris, T. D.; Brus, L. E. *Science* **1996**, *272*, 255.
(6) Shera, E. B.; Seitzinger, N. K.; Davis, L. M.; Keller, R. A.; Soper, S. A. *Chem. Phys. Lett.* **1990**, *174*, 553.
(7) Nie, S.; Chiu, D. T.; Zare, R. N. *Science* **1994**, *266*, 1018.
(8) Goodwin, P. M.; Ambrose, W. P.; Keller, R. A. *Acc. Chem. Res.* **1996**, *29*, 607.
(9) Zander, C.; Sauer, M.; Drexhage, K. H.; Ko, D.-S.; Schulz, A.; Wolfrum, J.; Brand, L.; Eggeling, C.; Seidel, C. A. M. *Appl. Phys. B* **1996**, *63*, 517.
(10) Fries, J. R.; Brand, L.; Eggeling, C.; Köllner, M.; Seidel, C. A. M. *J. Phys. Chem. A* **1998**, *102*, 6601.
(11) Vale, R. D.; Funatsu, T.; Pierce, D. W.; Romberg, L.; Harada, Y.; Yanagida, T. *Nature* (*London*) **1996**, *380*, 451.
(12) Ha, T.; Enderle, T.; Ogletree, D. F.; Chemla, D. S.; Selvin, P.; Weiss, S. *Proc. Natl. Acad. Sci. U.S.A.* **1996**, *93*, 6264.
(13) Schütz, G. J.; Schindler, H.; Schmidt, T. *Biophys. J.* **1997**, *73*, 1073.
(14) Weiss, S. *Science* **1999**, *283*, 1676.
(15) Bai, C.; Wang, C.; Xie, X. S.; Wolynes, P. G. *Proc. Natl. Acad. Sci. U.S.A.* **1999**, *96*, 11075.
(16) Peterman, E. J. G.; Brasslet, S.; Moerner, W. E. *J. Phys. Chem. A* **1999**, *103*, 10553.
(17) Ha, T.; Ting, A. Y.; Liang, W. B.; Caldwell, W. B.; Deniz, A. A.; Chemla, D. S.; Schultz, P. G. Weiss, S. *Proc. Natl. Acad. Sci. U.S.A.* **1999**, *96*, 893.
(18) Sako, Y.; Minoguchi, S.; Yanagida, T. *Nat. Cell Biol.* (*London*) **2000**, *2*, 168.
(19) Weiss, S. *Nat. Struct. Biol.* (*London*) **2000**, *7*, 724.
(20) Ambrose, W. P.; Moerner, W. E. *Nature* (*London*) **1991**, *349*, 225.
(21) Lu, H. P.; Xie, X. S. *Nature* (*London*) **1997**, *385*, 143.
(22) Ha, T.; Enderle, Th.; Chemla, D. S.; Selvin, P. R.; Weiss, S. *Chem. Phys. Lett.* **1997**, *271*, 1.
(23) Ying, L.; Xie, X. S. *J. Phys. Chem. B* **1998**, *102*, 10399.
(24) Yip, W.-T.; Hu, D.; Yu, J.; Vanden Bout, D. A.; Barbara, P. F. *J. Phys. Chem. A* **1998**, *102*, 7564.
(25) Weston, K. D.; Buratto, S. K. *J. Phys. Chem. A* **1998**, *102*, 3635.
(26) Weston, K. D.; Carson, P. J.; Metiu, H.; Buratto, S. K. *J. Chem. Phys.* **1998**, *109*, 7474.
(27) Köhn, F.; Hofkens, J.; De Schryver, F. C. *Chem. Phys. Lett.* **2000**, *321*, 372.
(28) Veerman, J. A.; Garcia-Parajo, M. F.; Kuipers, L.; van Hulst, N. F. *Phys. Rev. Lett.* **1999**, *83*, 2155.
(29) Weston, K. D.; Carson, P. J.; DeAro, J. A.; Buratto, S. K. *Chem. Phys. Lett.* **1999**, *308*, 58.
(30) English, D. S.; Furube, A.; Barbara, P. F. *Chem. Phys. Lett.* **2000**, *324*, 15.
(31) Ha, T.; Enderle, Th.; Chemla, D. S.; Selvin, P. R.; Weiss, S. *Phys. Rev. Lett.* **1996**, *77*, 3979.
(32) Ruiter, A. G. T.; Veerman, J. A.; Garcia-Parajo, M. F.; van Hulst, N. F. *J. Phys. Chem. A* **1997**, *101*, 7318.
(33) Bartko, A. P.; Dickson, R. M. *J. Phys. Chem. B* **1999**, *103*, 11237.
(34) Orrit, M.; Bernard, J. *Phys. Rev. Lett.* **1990**, *65*, 2716.
(35) Ambrose, W. P.; Moerner, W. E. *Nature* (*London*) **1991**, *349*, 225.
(36) Basché, T.; Kummel, S.; Bräuchle, C. *Nature* (*London*) **1995**, *373*, 132.
(37) Michler, P.; Imamoglu, A.; Mason, M. D.; Carson, P. J.; Strouse, G. F.; Buratto, S. K. *Nature* (*London*) **2000**, *406*, 968.
(38) Lounis, B.; Moerner, W. E. *Nature* (*London*) **2000**, *407*, 491.
(39) Tinnefeld, P.; Buschmann, V.; Herten, D.-P.; Han, K.-T.; Sauer. M. *Single Mol.* **2000**, *3*, 215.
(40) Sauer, M.; Drexhage, K. H.; Lieberwirth, U.; Müller, R.; Nord, S.; Zander, C. *Chem. Phys. Lett.* **1998**, *284*, 153.
(41) Knemeyer, J.-P.; Marmé, N.; Sauer, M. *Anal. Chem.* **2000**, *72*, 3717.
(42) Wazawa, T.; Ishii, Y.; Funatsu, T.; Yanagida, T. *Biophys. J.* **2000**, *78*, 1561.
(43) Herten, D.-P.; Tinnefeld, P.; Sauer, M. *Appl. Phys. B* **2000**,
(44) Becker, W.; Hickl, H.; Zander, C.; Drexhage, K. H.; Sauer, M.; Wolfrum, J. *Rev. Sci. Instrum.* **1999**, *70*, 1835.
(45) Eggeling, C.; Fries, J. R.; Brand, L.; Günther, R.; Seidel, C. A. M. *Proc. Natl. Acad. Sci. U.S.A.* **1998**, *95*, 1556.

(46) Tellinghuisen, J.; Wilkerson, C. W. *Anal. Chem.* **1993**, *65*, 1240.
(47) Tellinghuisen, J.; Goodwin, P. M.; Ambrose, W. P.; Martin, J. C.; Keller, R. A. *Anal. Chem.* **1994**, *66*, 64.
(48) Drexhage, K. H. Structure and Properties of Laser Dyes. In *Topics in Applied Physics: Dye Lasers*; Schäfer, F. P., Ed.; Springer-Verlag: Berlin 1973; Vol. 1, pp 144−178.
(49) Sauer, M.; Han, K.-T.; Müller, R.; Nord, S.; Schulz, A.; Seeger, S.; Wolfrum, J.; Arden-Jacob, J.; Deltau, G.; Marx, N. J.; Zander, C.; Drexhage, K. H. *J. Fluoresc*. **1995**, *5*, 247.
(50) Widengren, J.; Schwille, P. *J. Phys. Chem. A* **2000**, *104*, 6416.
(51) Lacoste, Th. D.; Michalet, X.; Pinaud, F.; Chemla, D. S.; Alivisatos, A. P.; Weiss, S. *Proc. Natl. Acad. Sci. U.S.A.* **2000**, *97*, 9461.
(52) Esa, A.; Edelmann, P.; Kreth, G.; Trakhtenbrot, L.; Amariglio, N.; Rechavi, G.; Hausmann, M.; Cremer, C. *J. Microscopy* **2000**, *199*, 96.
(53) Axelrod, D.; Hellen, E. H. In *Fluorescence Microscopy of Living Cells in Culture*; Tayler, D. L., Wang, Y. L., Eds.; Academic Press: San Diego 1989; Part B, pp 399−416.
(54) Enderlein, J. *Chem. Phys. Lett*. **1999**, *308*, 263.
(55) Basché, T.; Moerner, W. E.; Orrit, M.; Talon, H. *Phys. Rev. Lett.* **1992**, *69*, 1516.
(56) Asimov, M. M.; Gavrilenko, V. N.; Rubinov, A. N. *J. Lumin.* **1990**, *46*, 243.
(57) Menzel, R.; Thiel, E. *Chem. Phys. Lett.* **1998**, *291*, 237.
(58) Menzel, R.; Bornemann, R.; Thiel, E. *Phys. Chem. Chem. Phys.* **1999**, *1*, 2435.
(59) Bernard, J.; Fleury, L.; Talon, H.; Orrit, M. *J. Chem. Phys.* **1993**, *98*, 850.
(60) Wilkinson, F.; Leicester, P. A.; Ferreira, L. F. V.; Freire, V. M. M. R. *Photochem. Photobiol.* **1991**, *54*, 599.
(61) Weston, K. D.; Goldner, L. S. *J. Phys. Chem. B*. **2001**, *105*, 3453.
(62) Stracke, F.; Blum, C.; Becker, S.; Müllen, K.; Meixner, A. J. *Chem. Phys. Lett.* **2000**, *325*, 196.
(63) Sauer, M.; Han, K.-T.; Müller, R.; Schulz, A.; Tadday, R.; Seeger, S.; Wolfrum, J.; Arden-Jacob, J.; Deltau, G.; Marx, N. J.; Drexhage, K. H. *J. Fluoresc*. **1993**, *3*, 131.